Ionization in low-keV-energy Ar+Ar collisions*

F. J. Eriksen,† S. M. Fernandez,‡ A. B. Bray,§ and E. Pollack
Department of Physics, University of Connecticut, Storrs, Connecticut 06268
(Received 2 December 1974)

Ionization in Ar + Ar collisions is studied at beam energies of 2.00, 2.50, and 3.00 keV over an angular range from 2.0° to 12.0°. The ionization probability (P_1) shows a threshold for $\tau \approx 5$ keV deg and a second rise for $\tau \approx 25$ keV deg. The scattered ion beam is energy analyzed at selected energies and angles. For $2 < \tau < 12$ keV deg the ion energy-loss spectra show a double-peaked structure, at an 18-eV and at a 29-eV energy loss. At larger τ there is predominately one peak in the spectra at 43 eV. The energy losses and τ dependence of P_1 suggest that the 29- and 43-eV processes involve excitation of autoionizing states. Additional results at beam energies of 0.50, 0.75, 1.00, and 1.50 keV show $P_1(\tau)$ to be velocity dependent at these lower energies.

I. INTRODUCTION

In recent years a great deal of effort has been made to understand atomic collision processes in the low-keV energy region. Since a major fraction of the collisions in this energy range are inelastic, there has been a rapid development in inelastic collision theory, and it now appears that excitation at curve crossings of the quasimolecule can account for much of the observed scattering.

Currently several techniques are available for studying inelastic scattering, including electron and photon spectroscopy and energy-loss measurements on scattered ions and atoms.[1] Each of these methods has characteristic advantages and disadvantages. In electron and photon spectroscopy experiments there is generally some uncertainty about the states actually excited in a collision since cascade effects may contribute to the measured signal. In addition electron and photon spectroscopy experiments cannot provide information about R_0, the distance of closest approach in the collision. This is a particular disadvantage since both ionization and excitation processes are expected to be strong functions of R_0. Direct measurements on the scattered ions or atoms however are not complicated by cascade effects and do provide some information on R_0. On the other hand, electron and photon spectroscopy techniques are superior in energy resolution. In addition to effects resulting from finite angular resolution and from the motion of the target atoms, the unavoidable energy spread in the incident beam limits the ultimate resolution in scattered ion (or atom) energy-loss measurements. This spread does not affect the ejected-electron or photon studies since the cross sections are generally slowly varying functions of the incident beam energy. It should also be noted that the resolution of electron and ion energy analyzers is usually a fixed percentage of the electron or ion energy thereby allowing higher resolution in measurements on electrons since these energies are smaller than scattered ion energies. Finally, measurements by electron or photon spectroscopy techniques are limited to those collisions which result in the emission of an electron or photon. With the addition of time-of-flight techniques[1,2] for analyzing the energy of neutral scattered atoms, scattered ion or atom spectroscopy can, in principle, be used to study any inelastic process.

In this paper we study inelastic scattering, which results in ionization, in the Ar + Ar collision. Several studies of ionization have been made in the low-keV energy region.[3] Total-cross-section measurements were reported by Hayden and Amme[4] and Sluyters *et al.*,[5] while Gerber *et al.*[6] and Berry[7] have studied the energy distributions of the ejected electrons.

Ionization in the Ar + Ar system is of interest for several reasons. Most importantly, it can test the predictions of the Fano-Lichten[8] model for outer-shell electrons where it is not expected to hold. The Ar + Ar system can also serve as a guide in the construction of the electron energy curves for many-electron systems where configuration interactions are expected to be important.[9]

In the present experiment, ionization of fast Ar atoms by thermal Ar target atoms is studied at incident beam energies E_0, of 2.00, 2.50, and 3.00 keV. $P_1(E_0, \theta)$, the ionization probability is defined as the ratio $I(E_0, \theta)/T(E_0, \theta)$, where $I(E_0, \theta)$ and $T(E_0, \theta)$ are the scattered-ion and total signals respectively. $P_1(E_0, \theta)$ is determined for laboratory scattering angles θ from 2.0° to 12.0°. In addition the scattered ion beam is energy analyzed at selected angles and energies and the results indicate that most of the ionization is caused by the excitation of autoionizing states. To check for a velocity dependence in P_1, less detailed measure-

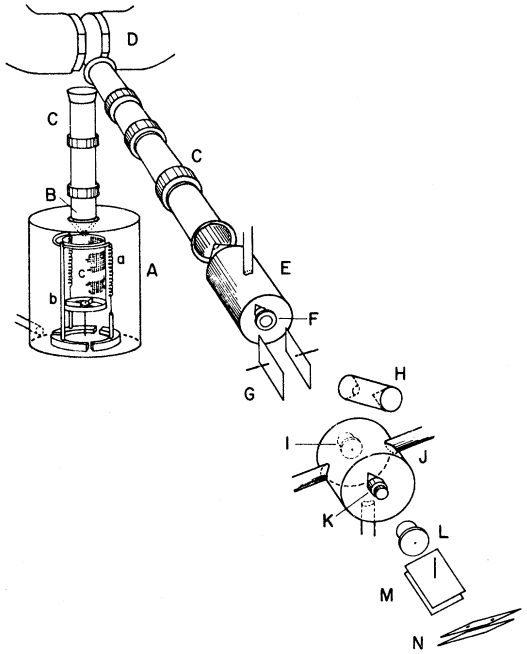

FIG. 1. Schematic diagram of the apparatus. Ion source (*A*), extractor (*B*), lenses (*C*), magnet (*D*), charge-exchange cell (*E*), collimating holes (*F*, *I*, *K*, *L*), ion deflector plates (*G*, *M*), Faraday-cup monitor (*H*), scattering chamber (*J*), electrostatic energy analyzer (*N*).

ments are made at incident beam energies of 1.50, 1.00, 0.75, and 0.50 keV.

II. APPARATUS

The apparatus has been previously described by Nagy *et al.*[10] and Savola *et al.*,[11] and is shown in Fig. 1. The only addition to the apparatus is a parallel plate electrostatic analyzer shown schematically in Fig. 2. Referring to Fig. 1, argon ions produced in the source (*A*) pass through the charge-exchange cell (*E*) where $\frac{1}{3}$ to $\frac{1}{2}$ of the beam is neutralized by resonant charge exchange in Ar gas. The resulting fast neutral beam enters the scattering chamber (*J*) through aperture (*I*). Apertures (*F*) and (*I*) define the incident beam collimation, while (*K*) and (*L*) define the detector collimation. Scattered particles passing through (*L*) then enter the energy analyzer (*N*) through slit S_1 (Fig. 2), and ions follow a curved trajectory toward slit S_2 when a potential difference V_a exists between the plates. Neutral atoms continue undeflected through slit S_3. Particles passing through S_2 or S_3 are detected by channeltron electron multipliers *C*1 or *C*2 respectively.

It is necessary to use two sets of collimation aperatures (*F*)–(*I*) and (*K*) and (*L*) in order to cover the range of scattering angles. If $\Delta\theta_S$ and $\Delta\theta_d$ are the half angles of the source [(*F*)–(*I*)] and detector [(*K*) and (*L*)] apertures, then for the large apertures $\Delta\theta_S = 0.47°$ and $\Delta\theta_d = 0.36°$, and for the small ones $\Delta\theta_S = 0.18°$ and $\Delta\theta_d = 0.12°$.

To verify that the apparatus is working properly, energy-loss spectra of scattered Ar^+ ions from $Ar^+ + Ar$ collisions are compared to those reported by Barat *et al.*[12] It is found that the differences in peak positions are within the uncertainty in the location of the peaks. In addition, measurements are taken using several ion-source gas pressures, several ion-source electron bombarding energies, and at different charge-exchange pressures. No effect on the data is observed. All data are taken under single-collision conditions.

III. EXPERIMENTAL PROCEDURE

For the $P_1(E_0, \theta)$ determinations slits S_1 and S_2 of the analyzer are fully opened (approximately 0.25 in. each). Standard electronic counting equipment is used to measure I, the number of ions reaching C_2 for N, a preset number of neutrals reaching C_1. In a run three values of I and N are determined at each E_0 and θ. To calculate P_1, the three I values are added together, the three N values added together and P_1 is the ratio $I/(I+N)$. Values of P_1 determined in the above way are averaged to obtain the reported $P_1(E_0, \theta)$.

Figures 3 and 4 show P_1 plotted as a function of τ, the reduced scattering angle (defined as $E_0\theta$). All data for Fig. 4 as well as for $\tau > 9$ keV deg in Fig. 3 are taken with the larger collimation. For $\tau < 9$ keV deg the data are taken with small collimation. Some data are taken at 1.50, 1.00, 0.75, and 0.50 keV (Fig. 3) to determine velocity effects. Of particular importance is that the P_1 values at 2.00, 2.50, and 3.00 keV fall nearly on a universal curve, with an inflection point in the curve at about 6 keV deg. A search is also made for scattered Ar^- and Ar^{++}, but these charge states are not found.

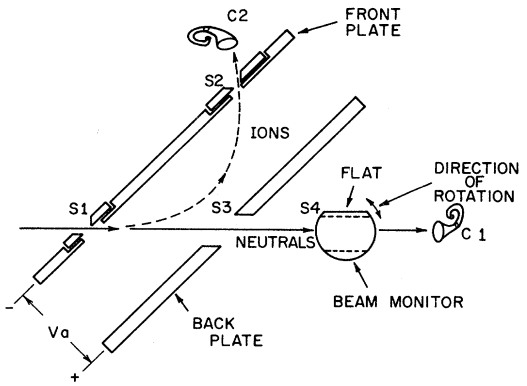

FIG. 2. Schematic diagram of the electrostatic energy analyzer.

To study the energy-loss spectra, slits S_1 and S_2 are narrowed to several thousandths of an inch. The neutral signal is routed to a control interface described by Bray *et al.*[13] The interface causes a change δV_a in the analyzer voltage whenever a preset number of neutral particles is accumulated. Simultaneously, the interface controls the channel of a multichannel analyzer (MCA) in which the number of arriving ions is recorded. In this way, the number of ions per preset number of detected neutrals (for analyzer voltage V_a) is stored in the MCA. The voltage V_a is continuously monitored by a digital voltmeter, and both the starting voltage and increment voltage δV_a are recorded for each run.

The energy profile of the incident beam is used to convert the applied analyzer voltage to kinetic energy of the scattered beam. If $\Delta V'$ represents the energy difference, in eV, between two features of a spectrum, then

$$\Delta V' = [E_0/V_a(E_0)]\Delta V \ , \qquad (1)$$

where E_0 is the incident beam energy in eV, $V_a(E_0)$ is the analyzer voltage at the peak of the incident beam energy profile, and ΔV is the difference in analyzer voltage between the two features of the spectrum.

The determination of the inelastic energy loss Q at each scattering angle requires knowing the kinetic energy of a particle elastically scattered at that angle. Unfortunately, the elastically scattered particles in Ar+Ar collisions are neutral. However, elastically scattered Ar^+ ions from Ar^++Ar collisions have basically the same energy as elastically scattered Ar from Ar+Ar collisions. The position of the elastic peak for Ar^++Ar collisions is determined for each Ar+Ar energy-loss profile. A typical pair of spectra are shown in Fig. 5. The zero position of the energy-loss scale is taken at the elastic peak in the Ar^++Ar spectrum.

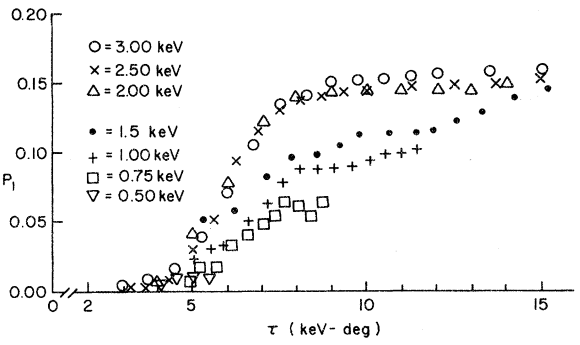

FIG. 3. Probability of ionization as a function of reduced scattering angle.

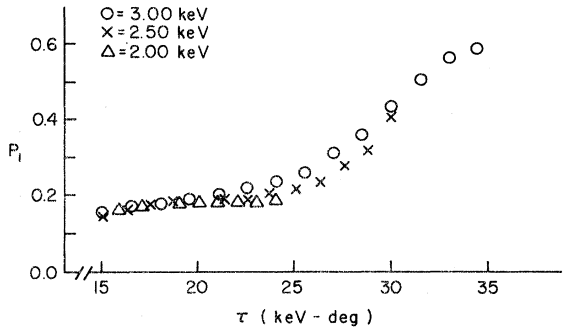

FIG. 4. Probability of ionization as a function of reduced scattering angle.

In order to obtain energy-loss data for θ greater than 4.0°, it is necessary to use rather wide slits for S_1 and S_2. The resolution under these circumstances is about 0.003 and several energy-loss profiles taken at 3.00 keV are shown in Fig. 6. The data show distinct peaks at 18, 29, and 45 eV, and possibly one at 60 eV. These peaks will be denoted by A, B, C, and D. As θ increases there is a clear evolution of the spectra toward larger inelastic energy losses. Higher-energy resolution, 0.001–0.002, is used in taking data for θ less than 4.0°. A double-peaked structure like that shown in Fig. 5 is found at all energies and angles investigated with this higher resolution. The average inelastic energy losses, as determined from spectra taken with the higher resolution are 18 eV for peak A and 29 eV for peak B.

IV. DISCUSSION

Peak A in the energy-loss spectra can only be explained by simple ionization of the projectile with no excitation of the resulting ion or of the target. The magnitude of peak A (in the higher-resolution data) is found to be at most 0.25 times that of peak B for $4 < \tau < 12$ keV deg. Because of this small ratio P_1 primarily reflects the behavior of peak B for these values. Peak A is found to become very small for $\tau > 18$ keV deg. Since 15.7 eV are required to ionize Ar I, the ejected electron has a 2.3-eV kinetic energy:

$$Ar + Ar \rightarrow Ar^+ + e^-(2.3\ \text{eV}) + Ar \quad (Q \approx 18\ \text{eV}) \ . \qquad (2)$$

The electron spectra should show this peak but unfortunately the measurements of Gerber *et al.*[6] are not made at sufficiently low electron energy. The number of ejected electrons is, however, seen to increase as the electron energy goes to zero. Berry's[7] measurements on the electron spectra are made for incident beam energies which are too low to allow a direct comparison

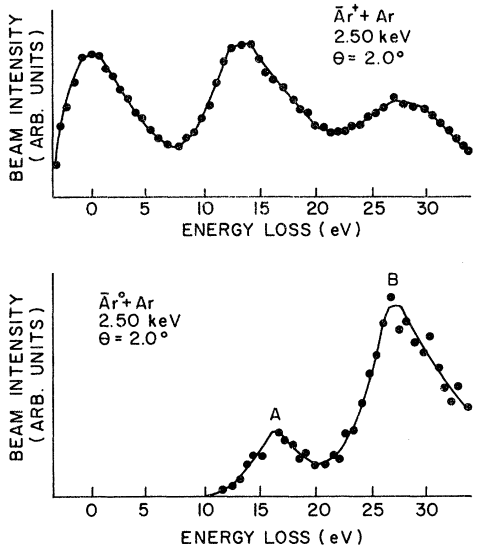

FIG. 5. Typical energy-loss spectra of Ar^+ from $Ar^+ + Ar$ and $Ar + Ar$ collisions.

with the present results.

The MO (molecular-orbital) correlation diagram[8] shown in Fig. 7 suggests several mechanisms which may be responsible for peak A. The $5f\sigma_u$ MO is seen to cross the $4s\sigma_g$ and $4p\pi_u$ MOs. Since the symmetry of the molecular wave function cannot change as a result of this collision, single-electron excitation is possible (via a rotational coupling) only to the $4p\pi_u$ MO. This transition excites one electron from its initial $3p$ atomic level to a final $4p$ level. The resulting collision products are $Ar(3p^5 4p) + Ar(3p^6)$ or $Ar^+(3p^5) + Ar^-(3p^6 4p)$. The Ar^- state lies in the continuum and decays by electron ejection with final collision products $Ar^+ + Ar + e^-$. Excitation of an electron from the $4d\sigma_g$ to $4s\sigma_g$ MO can also result in ionization. However, calculations by Sidis[14] show that the $4d\sigma_g$ MO is depressed in the region of interest and is therefore not likely to contribute to the observed ionization. Collisional excitation and ionization are also possible via an initial two-electron transition from the $5f\sigma_u$ to $4s\sigma_g$ MO. This type of process is discussed in detail in Ref. 2 and has been successful in accounting for the energy threshold of the total cross section for electron ejection in $Ar + Ar$ collisions.[4]

Peak B, corresponding to a Q value of 29 eV, has many possible explanations energetically. Processes involving ionization with concomitant excitation of the ion or target atom as well as processes involving projectile excitation to autoionizing states can produce a 29-eV energy loss. Figure 8 shows some of the autoionizing states which are known or expected to occur in Ar I. The states labeled a and b are from Ref. 6; c–e and g from Ref. 15; along with f and h from Ref. 16. As may be seen, excitation of two electrons from the $3p$ level to the $4s4p$ or $4s3d$ doubly excited states could produce ions having the measured 29-eV energy loss. In addition, core excited states may also contribute to the observed ionization. Since P_1 is dominated by peak B (at the smaller τ values) its threshold behavior, for $5 < \tau < 7$ keV deg, suggests an interaction occurring for values of R_0 between 0.75 and 0.70 Å (as calculated from a screened Coulomb potential[17] to allow comparison with Fig. 7). Core excited states and $4s3d$ excitation are thereby ruled out since the collisions are not sufficiently hard to reach the required distances of closest approach ($R_0 < 0.7$ Å) as may be seen on Fig. 7. The autoionizing states contributing to the observed ionization are therefore $4s4p$ and $4p^2$. The $4p^2$ excitation appears to be more

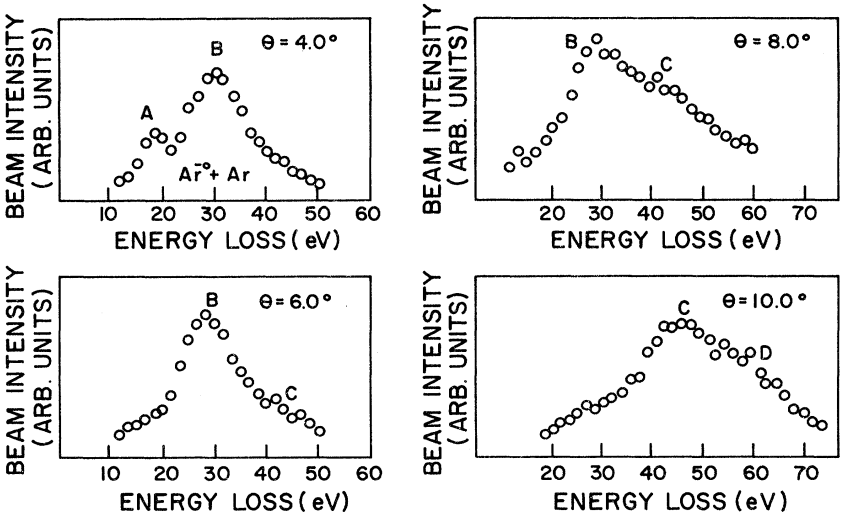

FIG. 6. Energy-loss spectra of Ar^+ from 3.0-keV $Ar + Ar$ collisions.

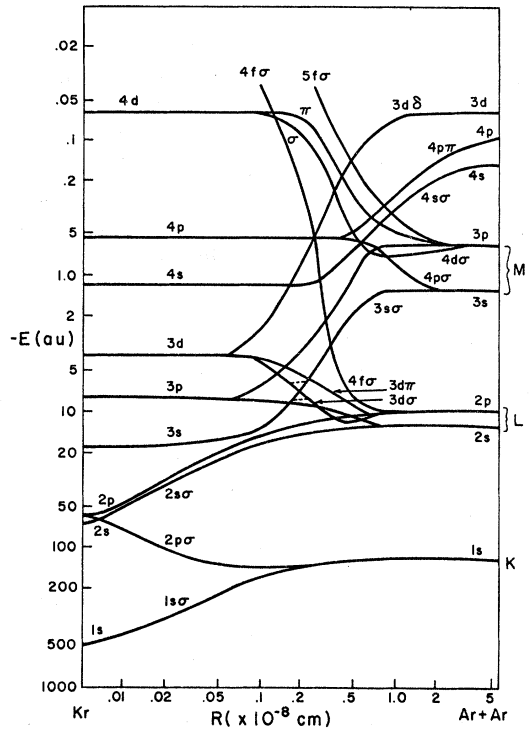

FIG. 7. Single-electron energy curves for Ar_2. The MO energies are from Ref. 8.

significant, however, on the basis of energy consideration.

Gerber *et al.*[6] report peaks in the electron spectra at 11.2, 11.5, 13.5, and 16.5 eV, which would correspond to energy losses of 26.9, 27.2, 29.2, and 31.2 eV in the present experiment. A broad peak in the ion spectra at 29 eV includes these energy losses, although the losses at 26.9 and 27.2 are not seen with very large probability. This discrepancy is explainable if the collisions which produce the 11.2- and 11.5-eV electrons do not fall in the τ range studied here.

Peak *C* at a 43-eV loss may be due to a variety of processes. Figure 6 shows energy-loss measurements at 3.00 keV for several scattering angles. Lower energy resolution is necessary here to allow measurements at large scattering angle. Peak *C* is seen to begin contributing to the ionization at a scattering angle of 6.0° and at 10.0° ($\tau = 30$ keV deg, $R_0 = 0.59$ Å[17]) it is the most important process. This process contributes to the change in slope of the P_1 vs τ plot (Fig. 4) at 25 keV deg, and to the large value of P_1 near 35 keV deg. Also of interest is that the P_1 vs τ curve is almost the same at the three energies presented, just as is found at these energies for the lower τ values (Fig. 3). This suggests that a curve-crossing mechanism is responsible for the additional ionization. A possible contributing process involves excitation of both a $3s$ and $3p$ electron:

$$\mathrm{Ar} + \mathrm{Ar} \rightarrow \mathrm{Ar}(3s3p^5nln'l') + \mathrm{Ar} \quad (Q > 44\ \mathrm{eV}) \ . \tag{3}$$

Madden *et al.*[15] have observed such states in the photoionization continuum of Ar I, and the excitation energy of these states lies between 44 and 58 eV. This range of energies would explain very nicely the broadness seen on the high-energy side of the 43-eV peak in the 3.00-keV 8.0° data, and especially in the 3.00-keV 10.0° data.

Although the MO energy-level diagram serves as a guide in interpreting experimental results, it is important to remember that the molecular potential-energy curves for the system should in fact be used. The potential-energy curves appropriate to process (3) are presently not known but

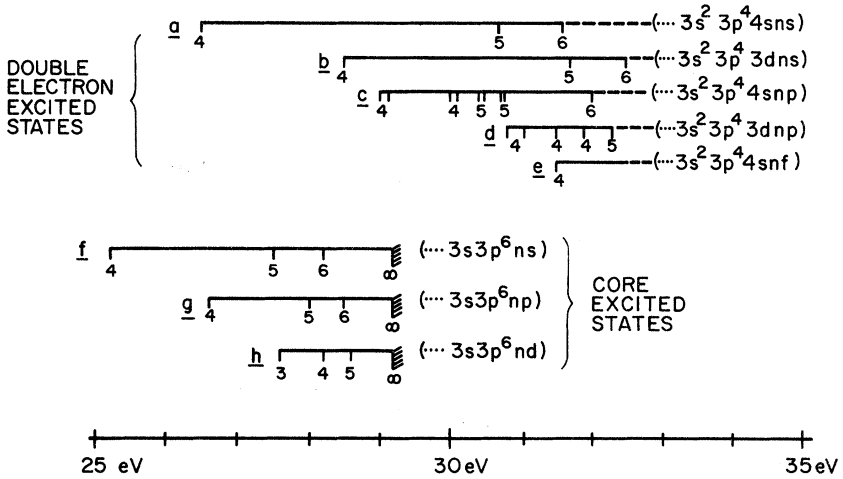

FIG. 8. Some autoionizing states of Ar. The states labeled *a* and *b* are from Ref. 6; *c*, *d*, *e*, and *g* from Ref. 15; *f* and *h* from Ref. 16.

as a starting point approximate curves can be constructed by adding the MO energies (Fig. 7) corresponding to a particular configuration. When this is done[18] for the excitation of $Ar(3s3p^5 4p^2)$, resulting from a $4p\sigma_u \rightarrow 4p\pi_u$ and $5f\sigma_u \rightarrow 4p\pi_u$ transition, the final state is found to cross the incident state at an internuclear separation of about 0.55 Å corresponding to a $\tau \approx 25$ keV deg.[17] The excitation of $Ar(3s3p^5 4s4p)$, from $4p\sigma_u \rightarrow 4p\pi_u$ and $4d\pi_g \rightarrow 4s\sigma_g$ MO transitions, is found to occur in the same τ region. It is interesting that although several approximations are used in determining the region of τ values contributing to the excitation, there is good agreement between these values and the experimental results (Fig. 4).

A hint of structure (peak D) is seen for $Q \approx 60$ eV at the largest τ values studied. A possible mechanism would involve the excitation of autoionizing states in both collision partners.

Excitations at curve crossing are seen to provide an explanation of the observed ionization in Ar-Ar collisions. There is still much to be learned from this collision system. Future measurements with higher-energy resolution as well as detailed studies of the velocity dependence are still necessary to guide the development of a refined theory for the general problem.

---

*Supported by the U. S. Army Research Office-Durham, the University of Connecticut Research Foundation, and the Connecticut Research Commission.

†Present address: Behlen Laboratory of Physics, University of Nebraska, Lincoln, Nebr. 68508.

‡Present address: Health Center, University of Connecticut, Farmington, Conn. 06032.

§Present address: Planning Systems Incorporated, McLean, Va. 22101.

[1]J. C. Brenot, J. Pommier, and M. Barat, J. Phys. B (to be published).

[2]J. C. Brenot, D. Dhuicq, J. P. Gauyacq, J. Pommier, V. Sidis, M. Barat, and E. Pollack, following paper, Phys. Rev. A 11, 1245 (1975).

[3]F. J. Eriksen, S. M. Fernandez, A. V. Bray, and E. Pollack, Proceedings of the Third International Conference on Atomic Physics, Abstract of Papers, Boulder, Colo., 1972, p. 70.

[4]H. C. Hayden and R. C. Amme, Phys. Rev. 141, 30 (1966).

[5]Th. J. M. Sluyters, E. de Haas, and J. Kistemaker, Physica (Utr.) 25, 1376 (1959).

[6]G. Gerber, R. Morgenstern, and A. Niehaus, J. Phys. B 6, 493 (1973).

[7]H. W. Berry, Phys. Rev. A 6, 1805 (1972).

[8]U. Fano and W. Lichten, Phys. Rev. Lett. 14, 627 (1965).

[9]M. Barat and W. Lichten, Phys. Rev. A 6, 211 (1972).

[10]S. W. Nagy, S. M. Fernandez, and E. Pollack, Phys. Rev. A 3, 280 (1971).

[11]W. J. Savola, Jr., F. J. Eriksen, and E. Pollack, Phys. Rev. A 7, 932 (1973).

[12]M. Barat, J. Baudon, M. Abignoli, and J. C. Houver, J. Phys. B 3, 230 (1970).

[13]A. V. Bray, F. J. Eriksen, S. M. Fernandez, and E. Pollack, Rev. Sci. Instrum. 45, 429 (1974).

[14]V. Sidis, M. Barat, and D. Dhuicq, J. Phys. B (to be published).

[15]R. P. Madden, D. L. Ederer, and K. Codling, Phys. Rev. 177, 136 (1969); R. P. Madden and K. Codling, Phys. Rev. Lett. 10, 516 (1963); R. P. Madden, D. L. Ederer, and K. Codling, Phys. Rev. 177, 136 (1969).

[16]C. E. Brion and L. A. R. Olsen, J. Phys. B 3, 1020 (1970).

[17]E. Everhart, G. Stone, and R. J. Carbone, Phys. Rev. 99, 1287 (1955).

[18]F. J. Eriksen, Ph.D. thesis (University of Connecticut, Storrs, Conn., 1975) (unpublished).